PLOS | COMPUTATIONAL BIOLOGY

RESEARCH ARTICLE

Binding of DNA-bending non-histone proteins destabilizes regular 30-nm chromatin structure

Gaurav Bajpai[1], Ishutesh Jain[1], Mandar M. Inamdar[2], Dibyendu Das[3], Ranjith Padinhateeri[1]*

1 Department of Biosciences and Bioengineering, Indian Institute of Technology Bombay, Mumbai, India, **2** Department of Civil Engineering, Indian Institute of Technology Bombay, Mumbai, India, **3** Department of Physics, Indian Institute of Technology Bombay, Mumbai, India

* ranjithp@iitb.ac.in

Citation: Bajpai G, Jain I, Inamdar MM, Das D, Padinhateeri R (2017) Binding of DNA-bending non-histone proteins destabilizes regular 30-nm chromatin structure. PLoS Comput Biol 13(1): e1005365. doi:10.1371/journal.pcbi.1005365

Editor: Alexandre V Morozov, Rutgers University, UNITED STATES

Received: December 5, 2016

Accepted: January 14, 2017

Published: January 30, 2017

Data Availability Statement: All relevant data are within the paper and its Supporting Information files.

Funding: We acknowledge financial support from Council of Scientific and Industrial Research India (Grant no.37(1582)/13/EMR-II to RP and 03 (1326)/14/EMR-II to DD) http://www.csir.res.in/, and Innovative Young Biotechnologist Award, Department of Biotechnology, Ministry of Science and Technology India (to RP) http://www.dbtindia.nic.in/funding-mechanism/awards/#4. The funders had no role in study design, data collection and

Abstract

Why most of the *in vivo* experiments do not find the 30-nm chromatin fiber, well studied *in vitro*, is a puzzle. Two basic physical inputs that are crucial for understanding the structure of the 30-nm fiber are the stiffness of the linker DNA and the relative orientations of the DNA entering/exiting nucleosomes. Based on these inputs we simulate chromatin structure and show that the presence of non-histone proteins, which bind and locally bend linker DNA, destroys any regular higher order structures (e.g., zig-zag). Accounting for the bending geometry of proteins like nhp6 and HMG-B, our theory predicts phase-diagram for the chromatin structure as a function of DNA-bending non-histone protein density and mean linker DNA length. For a wide range of linker lengths, we show that as we vary one parameter, that is, the fraction of bent linker region due to non-histone proteins, the steady-state structure will show a transition from zig-zag to an irregular structure—a structure that is reminiscent of what is observed in experiments recently. Our theory can explain the recent *in vivo* observation of irregular chromatin having co-existence of finite fraction of the next-neighbor ($i+2$) and neighbor ($i+1$) nucleosome interactions.

Author summary

The fate of a cell is not just decided by the genetic code but also by the nature of the 3D organization of the protein-bound DNA, known as chromatin. Chromatin packaging is believed to be in a hierarchical manner, and one of the crucial stages in the packaging is argued to be having a zig-zag structure with specific width of 30 nm. However, most of the recent experiments failed to find any zig-zag-like ordered arrangement of chromatin in living cells. In this work, we address this puzzle, and argue that any regular, ordered, packaging of chromatin is unviable given that certain types of proteins can bind and bend the chromosomal DNA.

analysis, decision to publish, or preparation of the manuscript.

Competing Interests: The authors have declared that no competing interests exist.

Introduction

In cells, DNA, with the help of a large number of proteins, is packaged into a higher order structure known as chromatin. In eukaryotes, in its simplest level of packaging, DNA is wrapped around histone proteins to form a "beads on a string" form of chromatin having a width ≈ 10 nm. The 'bead' here is a nucleosome—147 bp of DNA wrapped around an octamer-complex of histone proteins [1]. When the cells are preparing to divide, one observes that the DNA, with the help of many proteins, assumes a highly condensed structure. It is being thought that the 10-nm string of chromatin is further packaged in a hierarchical manner to produce this highly compact mitotic chromosome [1]. What this hierarchy of structures, if any, is and exactly how a DNA chain gets packaged into this highly compact form are interesting open questions [2–4].

Based on theoretical arguments and a few (mostly *in vitro*) experiments, it was proposed that the 10-nm chromatin string will fold itself into a higher order structure having an approximate width of 30-nm [5–7]. Some of the earliest theoretical models argued that the 30-nm chromatin should form a solenoid structure by coiling the known 10-nm fiber [5, 6]. However, later studies argued that the 10-nm chromatin should rather be arranged in a zig-zag fashion [8–12], which was subsequently supported by high resolution X-ray imaging of crystals made of tetra nucleosomes [13] and other *in vitro* biochemical studies of nucleosome arrays [14]. Since the zig-zag model is compatible with chromatin having a variety of linker DNA lengths, it became the most popular model for higher order structure, in the literature. However, contrary to all theoretical expectations and *in vitro* observations, experimental investigations could not prove the existence of 30-nm fibers *in vivo* [15–19]. Even though some experiments on chicken erythrocyte and starfish sperm chromatin, where non-histone proteins are very low, reported short-range zigzag structure [17, 20], detailed studies of chromatin in other nuclei, using Cryo-EM and synchrotron X-ray scattering methods, argued that the 30-nm structure is non-existent *in vivo*/*in situ* [21, 22]. A set of small angle X-ray scattering experiments concluded that 30-nm fibers are non-existent *in vivo*, and they could not find any particular lengthscale beyond 10 nm [22]. Neither in the interphase nor in the mitotic phase could experiments find any of the expected higher order packaging [21–24]. Why the theoretically predicted, and *in vitro*-observed, 30-nm fiber is elusive *in vivo* is a puzzle in the field of chromatin biology.

In this work, we address this puzzle of the 30-nm structure, based on basic biophysics principles involved in the packaging of chromatin. However, to get into the details, we need to understand the basic logic behind the proposed zig-zag structure of chromatin. We know a few facts: (i) DNA wraps around histone-octamer in nearly two turns such that the entry and exit segments of the DNA make a fairly restricted angle [25, 26] (see Fig 1). (ii) Linker DNA lengths (L_l) are in the range 20–60bp. (iii) DNA is a highly stiff elastic chain in the length scale below persistence length (L_p = 150bp) [10, 11, 27].

Since typically $L_l < L_p$, the linker DNA will be rigid and straight. Given that nearly 2 turns around histone-octamer would bring back the DNA to approximately the same side of the nucleosome where it entered, the combination of the two factors—entry/exit angle and stiff linker region—would give rise to a preferred structure like a zig-zag (see Fig 1b). There have been experimental studies that have indicated the occurrence of straight linker regions [10, 11] and restricted entry/exit angles [25, 26] in zig-zag chromatin. All other constituents (ions, low-salt buffer conditions, linker histones) can be thought of as agents influencing these two factors [28–33].

Even though the entry/exit angle and DNA rigidity have been the primary argument supporting zig-zag structure, this neglects a couple of facts: (i) *in vivo*, non-histone proteins can

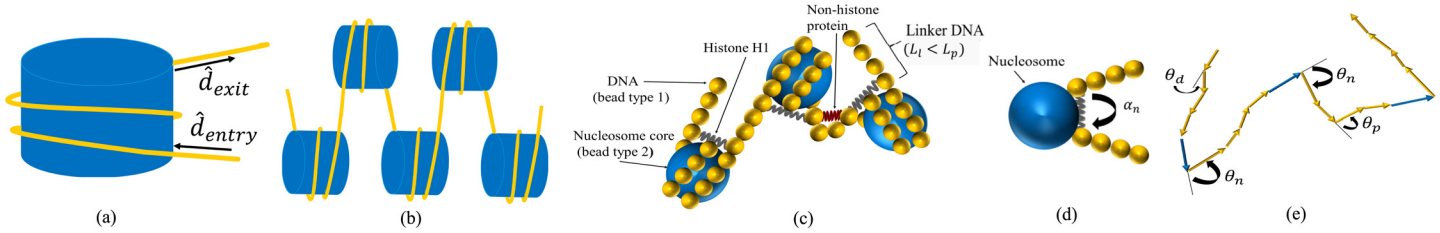

Fig 1. (a) When the DNA (yellow chain) is wrapped around the histone octamer (blue), we can represent the direction of the DNA segments that enters and exits the histone core as two vectors as shown here. The relative orientations of these entry/exit vectors will influence the local structure of the chromatin. (b) Linker DNA is typically rigid and straight. Rigid linker DNA and restricted orientations of entry/exit DNA segments will promote a zig-zag structure. (c–d): Schematic diagram describing the models: (c) Bead-spring model—DNA is modelled as a polymer made of beads of type-1 (yellow). 14 DNA-beads wrap around the histone-octamer bead (type-2, blue) to form a nucleosome. The picture also depicts linker histone H1 constraining entry/exit DNA beads (black spring), non-histone protein bending the linker region (red spring), and rigid linker regions when it is free of non-histone proteins. (d) Equivalently, nucleosome is considered as a bead that constraints the entry/exit DNA segments at an angle α_n. (e) FRC model—chromatin is modelled as a long 3D chain of N vectors. Yellow vectors represent linker DNA segments, which make a small angle θ_d with respect to its neighbor vector (in the absence of a non-histone protein); blue arrows represent histone-bound DNA having an angle $\theta_n = \pi - \alpha_n$ between them. When a non-histone protein is present in the linker region, yellow tangents make a relative angle of θ_p as shown.

doi:10.1371/journal.pcbi.1005365.g001

bind on the linker region and distort the orientation. For example, highly abundant high mobility group (HMG) proteins (e.g., nhp6 in yeast), and many other architectural transcription factors are known to bend DNA [34–38]. This bending by non-histone proteins can potentially affect the structure of chromatin. (ii) Since DNA has a nonlinear bending elasticity, it can have flexible hinges [39–43]. Given that DNA bending due to non-histone proteins is a certainty, it is important to consider them in any model that investigates the chromatin structure *in vivo*. Existing models primarily predict zig-zag or solenoid-like structures [44–46]. Recent models also predict polymorphic structures based on the variation in nucleosome repeat lengths [32, 47]. However, none of the existing papers, to the best of our knowledge, have accounted for the effect of local DNA curvatures resulting from non-histone protein binding and/or the possibility of highly flexible regions due to other factors. Neither have these studies systematically investigated how the chromatin structure would appear when a large number of nucleosomes (beyond 100 nucleosomes) are present in the presence of DNA-bending proteins.

In this work we study the higher order folding of nucleosome-bound DNA taking into account the possibility of non-histone proteins binding along the linker region, bending the DNA locally. Performing extensive simulations with two different models for chromatin, we show that (i) in the absence of non-histone protein binding, the nucleosome-bound DNA folds into a regular zig-zag structure; (ii) after the introduction of the non-histone proteins that bend linker DNA, the regular zig-zag structure starts disappearing. We compute the chromatin structure in the presence of specific proteins such as nhp6 and HMG. As a function of the density of bound non-histone proteins, we find that there is a transition from a zig-zag structure to an irregular higher order structure. We also investigate the influence of linker length on the formation of irregular structures.

Materials and methods

To investigate the role of DNA-bending proteins in higher order chromatin structures, we performed two kinds of simulations: (i) Brownian dynamics (BD) simulations considering a bead-spring model of DNA and accounting for nucleosome and proteins explicitly, and (ii) Monte Carlo (MC) simulations considering a freely rotating chain (FRC) model for chromatin.

Bead-spring model

In the first model (Fig 1(c)), DNA is considered as a polymer chain of N beads of type-1 (small, yellow beads) connected by linear springs of stiffness k_s. Bending elasticity of DNA is introduced using the worm like chain model (see details in the following text). The system we simulate has M nucleosomes where each nucleosome is created by wrapping 14 beads of DNA (=147 bp) in ≈ 1.7 turns (8 beads per wrap) around a second type of bead (histone core particle bead, blue, Fig 1(c)). The DNA-nucleosome interaction is accounted for by connecting the 14 beads via another set of linear springs having stiffness k_n. Linker histones (H1) are modeled as another type of spring connecting DNA segments that enter/exit nucleosomes. Two nucleosomes, when they are closer than a prescribed cut-off distance, can interact with each other; in the model, this inter-nucleosome interactions are also approximated as spring forces between two histone core particles. An important addition in the model is the presence of DNA-bending non-histone proteins—we assume that non-histone proteins can bind in the linker regions and bend the DNA locally. To mimic this, we consider non-histone protein as a spring that will connect two DNA-beads in the middle of the linker region and bring them together (see Fig 1(c), red); the net result is bending of the linker DNA. As mentioned earlier, the stretching energy of DNA (U_s), the DNA histone interaction energy (U_n), the linker histone interaction energy (U_l), the interaction energy of the non-histone protein (U_p), and the inter-nucleosome interaction energy (U_h) are approximated using a quadratic potential with different stiffnesses (k_α) and equilibrium extensions (r_α) as:

$$U_\alpha = \frac{k_\alpha}{2}\sum_{i,j}(|\mathbf{r}_i^{(\beta)} - \mathbf{r}_j^{(\gamma)}| - r_\alpha)^2 \tag{1}$$

where $\alpha \in \{s, n, l, p, h\}$, β and γ are symbols indicating whether the bead is a DNA-bead ($\mathbf{r}_i^{(1)}$) or a nucleosome bead ($\mathbf{r}_i^{(2)}$). (i) For DNA chain $\alpha = s$, $\beta = \gamma = 1$, $j = i+1$ and i ranges from 1 to $N - 1$. (ii) For nucleosome core-DNA interaction $\alpha = n$, $\beta = 2$, $\gamma = 1$, i ranges from 1 to M and j takes 14 values, for each i, representing the identity of the correspoding histone-bound DNA beads. Since nucleosomes are not dynamic in our study (no sliding or disassembly of nucleosomes), we have also prepared the system, equivalently, replacing the nucleosome as an effective bead with $U_n = k_n^{\text{eff}}\sum_i 1 - \cos(\alpha_i - \alpha_n)$ which constraints the DNA entering and exiting the nucleosome at an angle at α_n(see Fig 1(d)) [48]. This saves computational time and allows us to run BD simulations for a longer chromatin. (iii) For linker histone interaction $\alpha = l$, β and γ represent the entry and exit DNA beads, respectively, $j = i$ and i ranges from 1 to $M - 1$. (iv) For non-histone protein binding at the linker region $\alpha = p$, β and γ represent the identity of the location where non-histone proteins bind; i goes from 1 to v, $j = i + 3$, where v is the total number non-histone proteins bound. Different non-histone proteins will have different r_p values representing the bending angles they induce, as we discuss later in the manuscript (also see Supporting Information (SI) S1 Text and S1 Fig). (v) For inter-nucleosome interaction $\alpha = h$, $\beta = \gamma = 2$; at every instant i and j are computed such that the i^{th} nucleosome can interact with the j^{th} neighbor positioned below a certain cut-off distance = $9a$. When two nucleosomes are beyond this cut off distance, the inter-nucleosome interaction energy of the pair is zero. Since inter-nucleosome interactions are dominated by histone tails, and since nucleosomes have only finite number of tails, we assume that each nucleosome interacts only with two nearby nucleosomes ($j \leq 2$) (We have also done simulations accounting for more than two tails). To mimic the steric hindrance of

DNA beads, the repulsive part of the standard Lennard-Jones (LJ) potential (U_{LJ}) is used (when $|\mathbf{r}_i^{(1)} - \mathbf{r}_j^{(1)}| < 2a$) such that

$$U_{LJ} = \epsilon \sum_{\substack{i=1 \\ j>i}}^{N-1} \left[\frac{(2a)^{12}}{(|\mathbf{r}_i^{(1)} - \mathbf{r}_j^{(1)}|)^{12}} - 2\frac{(2a)^{6}}{(|\mathbf{r}_i^{(1)} - \mathbf{r}_j^{(1)}|)^{6}} + 1 \right] \tag{2}$$

where ϵ is potential well depth. The energy is zero when $|\mathbf{r}_i^{(1)} - \mathbf{r}_j^{(1)}| \geq 2a$ The bending energy (U_b) of the DNA chain is given by

$$U_b = \frac{k_b}{2a} \sum_{i=1}^{N-1} (1 - \cos\theta_i) \tag{3}$$

where k_b is the bending stiffness of DNA and θ_i is the angle between two nearby bonds in the bead-spring model. The total energy of the chromatin in this model is given by $U_{tot} = U_s + U_{LJ} + U_b + U_l + U_n + U_p + U_h$. Since expanding any potential energy close to its stable minimum gives us a quadratic function, we assumed a harmonic nature for most of our interactions. However, we have also done simulations with other functional forms (e.g, Morse potential) to ensure that the results are robust (see S1 Text). The system, accounting for all potentials, is simulated using BD by solving the equation given by

$$\frac{d\mathbf{r}_i^{(\gamma)}}{dt} = -\mu_0^{(\gamma)} \nabla_{\mathbf{r}_i^{(\gamma)}} U_{tot}(t) + \boldsymbol{\xi}_i^{(\gamma)}(t) \tag{4}$$

where $\gamma = 1$ or 2 represents the identity of the beads, namely the DNA beads and nucleosome core particles, respectively. μ_0 is the mobility, and $\boldsymbol{\xi}_i$ is the thermal noise experienced by each particle such that $\langle \boldsymbol{\xi}_i \rangle = 0$ and $\langle \boldsymbol{\xi}_i(t) \cdot \boldsymbol{\xi}_j(t') \rangle = 6k_B T \mu_0 \delta_{ij} \delta(t - t')$ (see [50] for details). Given an initial condition, we solve the equation taking a set of parameters as discussed in the following text. We have also done simulations with standard simulator tool LAMMPS to ensure robustness of our results [51](see S1 Text). From the simulations, we obtain the positions of all beads as a function of time ($\mathbf{r}(t)$); when the system equilibrates we sample shapes of the chromatin and compute different quantities as discussed in the Results section.

Parameters used in BD simulation

The basic length scale is taken as one helical repeat of DNA 10.5 bp, which is also the diameter of the DNA bead ($2a$) and the equilibrium distance of the DNA spring (r_s). The bending stiffness of DNA is $k_b = 50\ k_B$T nm where $T = 300$ K, and k_B is the Boltzmann constant [32]. Since, within this model, we want to hold the interacting DNA nearest-neighbor beads, DNA-nucleosome beads, and DNA-protein spring unstretchable, we took the corresponding stiffness values to be very high: $k_s = k_n = k_p = 100k_BT/r_s^2$. We have taken the linker histone interaction constant k_l in the range 30 to $100k_BT/r_s^2$ and $k_n^{\text{eff}} = 50k_BT$. For the purpose of this work, the exact value of these stiffness parameters are irrelevant as long as they are high enough to reduce large fluctuations (see S1 Table). Based on the literature and various geometrical constraints in the problem, we take $r_n = 8r_s/\pi$, $r_l = 2.5r_s$, and $r_h = 4.2r_s$ [32]. We consider effects different specific non-histone proteins by varying value of r_p. Since highly abundant proteins like nhp6 (yeast) and HMG-B are known to bend DNA making bend angles of $\approx 90^\circ$ or $\approx 120^\circ$ [52, 53], we chose values $r_p = 2.4r_s$ and $r_p = 2r_s$ such that the appropriate angles are formed (see S1 Text for more information). The timescales and mobility parameters are taken as $\Delta t =$ 0.04ns, $\mu_0^{(1)} = 2 \times 10^{-4} r_s/k_BT\Delta t$, and $\mu_0^{(2)} = 1.5 \times 10^{-4} r_s/k_BT\Delta t$ respectively (see S2 Table for details on non-dimensionalization of some of these parameters). We run the simulations for a

time (0.04s) which is much longer than the time it takes for the system to reach a steady state (milliseconds) having constant mean energy and radius of gyration.

FRC model

To understand how chromatin is structured *in vivo*, one needs to simulate a long chromatin having a large number of nucleosomes (thousands of nucleosomes) in a large parameter space. Since it is computationally intensive to do so using BD simulations (typical BD simulations simulate <100 nucleosomes), a freely rotating chain model for the chromatin is employed. In the FRC model, we consider chromatin as a long 3D chain made of N tangent vectors. Orientations of the vectors are chosen such that the angle between the vector i and $i-1$ is θ_i (see Fig 1(e)). If the i^{th} vector is a DNA vector, it makes a relative angle of $\theta_i = \sqrt{4a/L_p}$ with its neighbor [54]. As per the definition of FRC, the rotation angle ϕ is chosen randomly [54]. From a structural point of view, it can be argued that binding of the histone-complex (or any protein) constrains DNA subunits entering and exiting the histone octamer (protein) [26]. Therefore, if the i^{th} bead in the FRC is a nucleosome, a relative angle of $\theta_i = \frac{2\pi}{3}$ is assigned between the two adjacent tangents [25]. The corresponding ϕ_i angle is chosen in a range of -10° to 10° randomly so as to satisfy the known zig-zag structure seen in earlier simulations. We also introduced the DNA-bending non-histone proteins in the FRC as follows. While constructing the FRC, at every linker region, one neighboring vector pair in the middle is chosen with a given probability ρ, and imposed a certain angle θ_p representing the binding activity of non-histone proteins. First we consider bending due to specific proteins like nhp6 and HMG-B ($\theta_p \approx 90^\circ$ and 120°) [52, 53] and then we do a calculations considering a distribution of angles around these typical values. The angle ϕ here is chosen randomly between -10° and 10°. In this manner, we constructed a large number of chromatin configurations (many realisations), each having 2000 nucleosomes. To quantify the structure of these configurations we calculated $I(k)$ which is the probability that any nucleosome is in "contact" with its k^{th} neighbor [32] (see S2 Text for details). Two nucleosomes are defined to be in contact when the distance between them is below a cut-off distance of 16 nm ($9a$), which is the estimated mean length of histone tail interactions.

Results

First, we present the results from BD simulations. In Fig 2, we present the structure of chromatin (3D positions of nucleosomes and linker DNA) having M = 20 nucleosomes, and uniform linker length of 42 bp. In the absence of any non-histone proteins that bend the linker region, we get a nice zig-zag structure (Fig 2a; also see S2 Fig). For convenience, we used a color code by which one can see how odd (blue) and even (green) nucleosomes are nicely separated in a zig-zag fashion such that the i^{th} nucleosome is close to the $(i+2)^{nd}$ nucleosome (Fig 2a). However, once we introduce some amount of non-histone proteins that bind on the linker region and bend it locally($\rho = 0.5$), the zig-zag structure is destroyed and an irregular structure emerges. Note that the colors are now mixed indicating the loss of any regular arrangement.

To characterize these structures, we computed the corresponding contact probabilities $I(k)$ [32]. In the absence of any non-histone protein binding, $I(k)$ peaks at $k = 2$ (Fig 2c). This means that most of the nucleosomes are in contact with their next neighbor. This is the signature of a typical zig-zag structure. Given that linker DNA regions are nearly straight, the zig-zag structure is maintained for various values of inter-nucleosome interaction parameters—different curves represent different inter-nucleosome interaction parameter (non-dimensionalized $\tilde{k}_h = 2k_h a^2/k_B T$) values. We then computed $I(k)$ in the presence of non-histone proteins

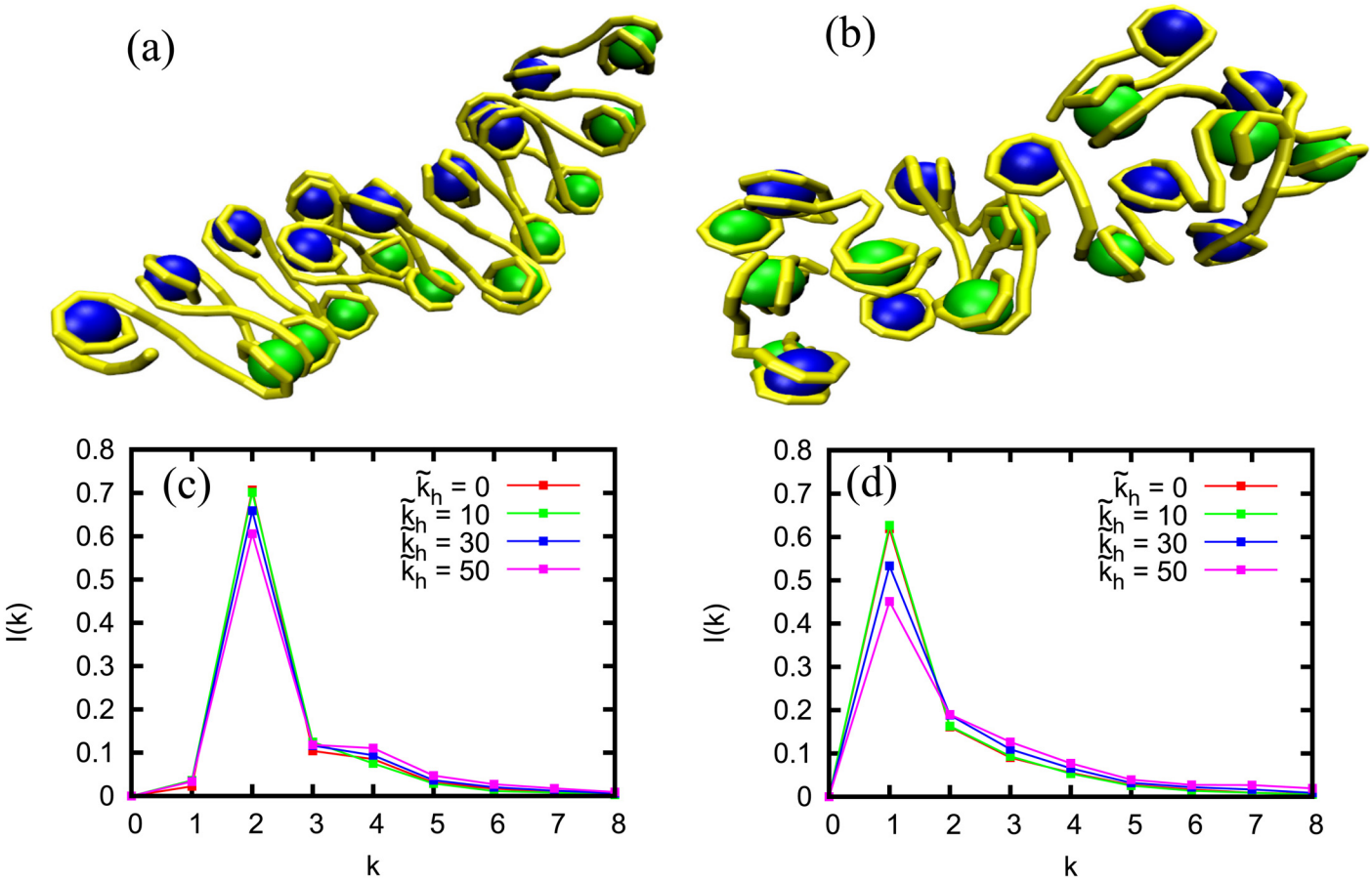

Fig 2. (a–b): Snapshots of chromatin from BD simulations showing DNA (yellow) and nucleosomes (blue and green) [55]. (a) In the absence of non-histone proteins; a zig-zag structure is seen. (b) In the presence of non-histone proteins that bend linker DNA (density $\rho = 0.5$). DNA-bending brings neighbouring nucleosomes closer to each other mixing the blue and green. This destroys the zig-zag nature where, typically, next neighbors (same-color nucleosomes) are closer than the neighbors (different colors). Both have inter-nucleosome interaction with $\tilde{k}_h = 50$. (c–d): $I(k)$ from BD simulations. (c) Without ($\tilde{k}_h = 0$) and with inter-nucleosome interactions ($\tilde{k}_h = 10, 30, 50$) and in the absence of any non-histone protein. Here $I(k)$ peaks at $k = 2$ indicating the formation of zig-zag structure for each $\tilde{k}_h$. (d) Without ($\tilde{k}_h = 0$) and with inter-nucleosome interactions ($\tilde{k}_h = 10, 30, 50$) in the presence of non-histone proteins($\rho = 0.5$). Here the peaks at $I(1)$ imply that neighboring nucleosomes are geometrically close to each other, and the zig-zag structure is dismantled in the presence of non-histone proteins.

doi:10.1371/journal.pcbi.1005365.g002

that distort linker DNA. The results are shown in Fig 2d for different inter-nucleosome interactions and 50% density of bound non-histone proteins. The $I(k)$ is no more peaked at $k = 2$; the peak is shifted to $k = 1$, indicating the destruction of the zig-zag structure. For higher inter-nucleosome interactions (different curves), two nucleosomes come very close and the overall structure is more tightly packed. The peak probability decreases slightly with higher interactions as more and more far away neighbors get locked within the cut off distance. These results indicate that the presence of DNA-bending non-histone proteins can be a crucial factor in determining the chromatin structure at the length scale of a gene, and may plausibly explain why the 30-nm higher order structure is elusive under in vivo conditions (also see S3 and S4 Figs). To test whether the precise model for linker histone would affect our results, we did a set of simulations considering linker histone as a bead that interacts with two entry/exit linker DNA and the corresponding nucleosomes as suggested by data in the literature [49] (see S1 Text). Results in S5 Fig show that this does not change our findings. We also did BD

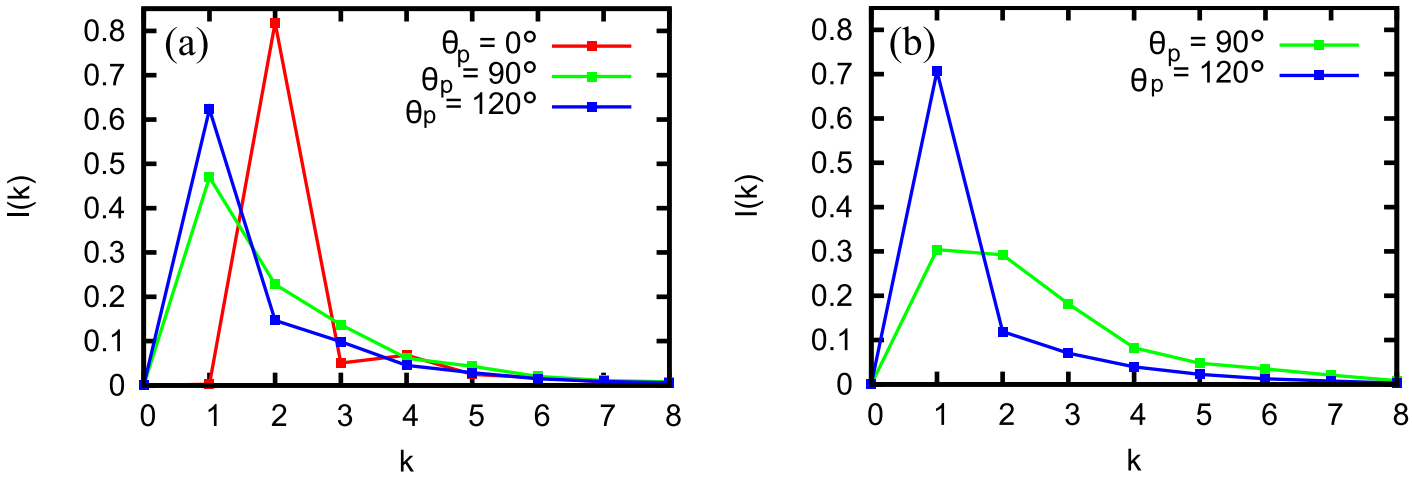

Fig 3. BD simulation with two specific DNA-bending geometries corresponding nhp6 and HMG-B. (a) $I(k)$ for proteins having a size of 20bp (one angle involving 2 bonds in the model) with bending angle = 120˚ (blue) and 90˚ (green). The red curve is the control when there is no DNA-bending protein. (b) For proteins having a size of 30bp (one angle involving 3 bonds in the model; see S1 Text). The plots are for $\tilde{k}_b = 50$ and $\rho = 0.5$ and with nucleosomes as angles $\alpha_n = 60^\circ$ done using LAMMPS [50]. In all the cases, the presence of DNA-bending proteins shifts the peak away from $k = 2$ indicating the destruction of zig-zag.

doi:10.1371/journal.pcbi.1005365.g003

simulations considering nucleosomes as angle-inducing proteins (Fig 1(d); see the following text). This also gives us similar results as above.

Specific proteins with different DNA-bending angles and sizes

We investigated the role of specific DNA-bending proteins in determining the structure of chromatin using the above BD simulations. DNA-bending protein in yeast nhp6 is reported to bend DNA making angles of $\theta_p \approx 120^\circ$ [52, 56] or $\approx 90^\circ$ [52, 57]. The HMG-B protein is reported to bend DNA making $\theta_p = 90^\circ$ [53, 58]. The proteins are typically known to have a size (footprint on DNA) of $\approx 20bp$ (HMG-B, nhp6; bend involving 2 bonds) or $\approx$ 30bp (some proteins in the HMG family; bend involving 3 bonds) [58, 59]. In Fig 3 we present our results in the presence of nhp6 and HMG-B proteins bending DNA with angles $\theta_p = 90^\circ$ and 120˚. In the absence of any protein($\theta_p = 0$), I(k) peaks at $k = 2$ indicating zig-zag (Fig 3 (a)). When we introduce nhp6 or HMG-B having DNA-bending angle of 90˚, size = 20bp, we get a peak at $k = 1$ (green curve). The peak at $k = 1$ becomes more dominant if the bending angle increases to 120˚ (blue curve). For larger proteins (size 30bp) too we see that the zig-zag structure is destroyed (Fig 3(b), peak is not at $I(2)$). All the above results are for a protein density of $\rho = 0.5$ per linker region, which is close to the known abundance of the DNA-bending non-histone proteins [35]. see S6, S7 and S8 Figs for more angles and parameters. We also performed simulations with different types of inter-nucleosome interactions by varying the strength of the interactions and the nature of the potential (see S3, S4 and S9 Figs).

To get an intuitive understanding of the above results, we performed simple 2D simulations using the FRC model as discussed in the text earlier. We simulated the structure of a chromatin having 24 nucleosomes, with uniform linker length of 42 bp, and the results (XY position nucleosomes and linker DNA) are plotted in Fig 4. In the absence of non-histone proteins, the structure is a clear zig-zag (Fig 4a). When we add non-histone proteins that bind along the linker region and bend the linker DNA, beyond a critical density of bound non-histone proteins, we completely lose the zig-zag nature and obtain a chromatin with irregular structure

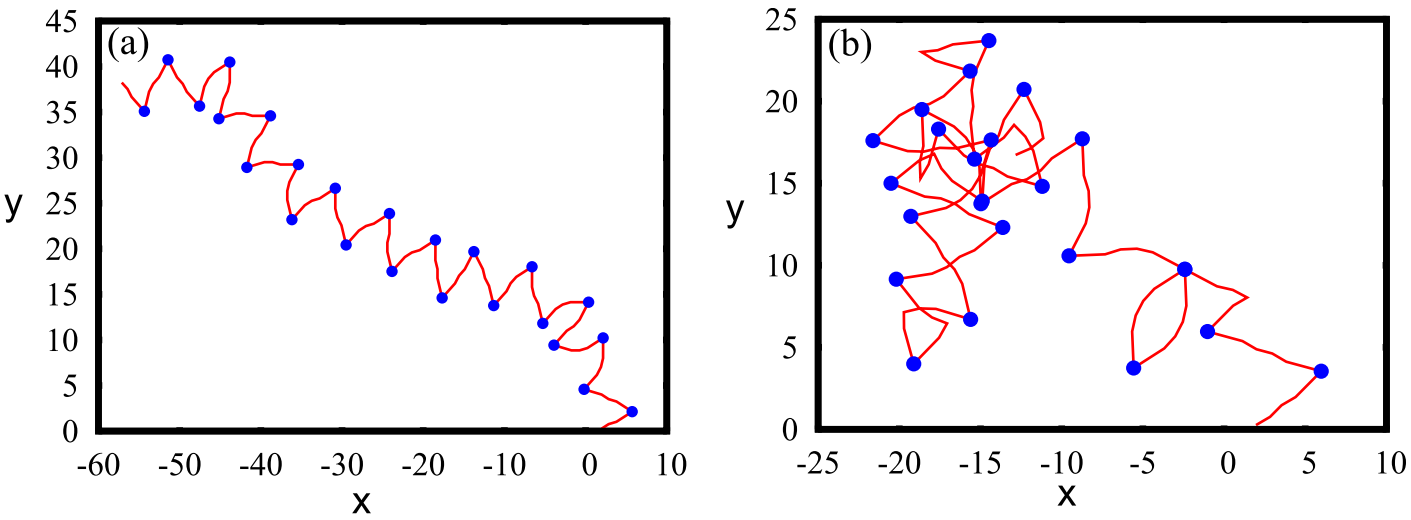

Fig 4. Snapshots of chromatin simulated using the FRC model in 2D showing linker DNA (red) and nucleosomes (blue). The linker length is ≈ 42 bp. (a)In the absence of any non-histone protein, we get a nice zig-zag-like structure. (b)In the presence of non-histone proteins where each linker region has a probability of 0.24 for non-histone protein to bind. The presence of non-histone proteins is modeled as a bend in the linker region. The non-histone proteins (not marked separately) are visible as sharp angles between two neighboring blue dots.

doi:10.1371/journal.pcbi.1005365.g004

(Fig 4b, $\rho = 0.24$, $\theta_p = 120^\circ$ with random orientations). This simple numerical study supports the hypothesis that the role of non-histone proteins is crucial in deciding the higher order structure of chromatin.

Large-scale chromatin organization

So far we did simulations with a small number of nucleosomes ($M \approx 20$, approximate length scale of a single gene). However, what will be the chromatin organisation in the longer length-scale (length scale of many genes) accounting for a large number of nucleosomes is an important question. Since performing BD for large systems is computationally expensive, and since both BD and FRC simulations give similar results, we implemented the 3D FRC model to probe large-scale organization of chromatin. Using the FRC model, we generated a large number of ($\approx 10^7$) equilibrium configurations of chromatin, each having 2000 nucleosomes, both with and without non-histone proteins. Systematically varying protein density (ρ), we investigated the amount of non-histone proteins required for the appearance of an irregular structure. To compare the 3D FRC model with and without proteins and to quantify the resulting nucleosome organization in space, here too we computed I(k) (Fig 5a). In the absence of non-histone proteins (Fig 5a, blue), the peak is at $k = 2$ implying a zig-zag structure. As protein density (ρ) increases, the $k = 2$ becomes less probable, and the probability of finding $k \neq 2$ increases. Here the bending angle of non-histone protein is chosen as $\theta_p = 90^\circ$ representing proteins like HMG-B or nhp6 [52, 53].

Results presented in Fig 5a suggest that, as a function of one parameter—non-histone protein density—there exists a transition from a zig-zag structure (dominant peak is at $k = 2$) to an irregular structure (dominant peak at $k \neq 2$). The plot of peak position (the value of k at which $I(k)$ peaks) as a function of protein density (Fig 5a, inset) captures this transition and shows that the transition happens when the protein density is ≈0.48. This is also the parameter regime where $I(1)$ is comparable to $I(2)$—this is important since recent experiments have indicated that chromatin has an irregular structure, and at the same time there exist both $i/i + 1$

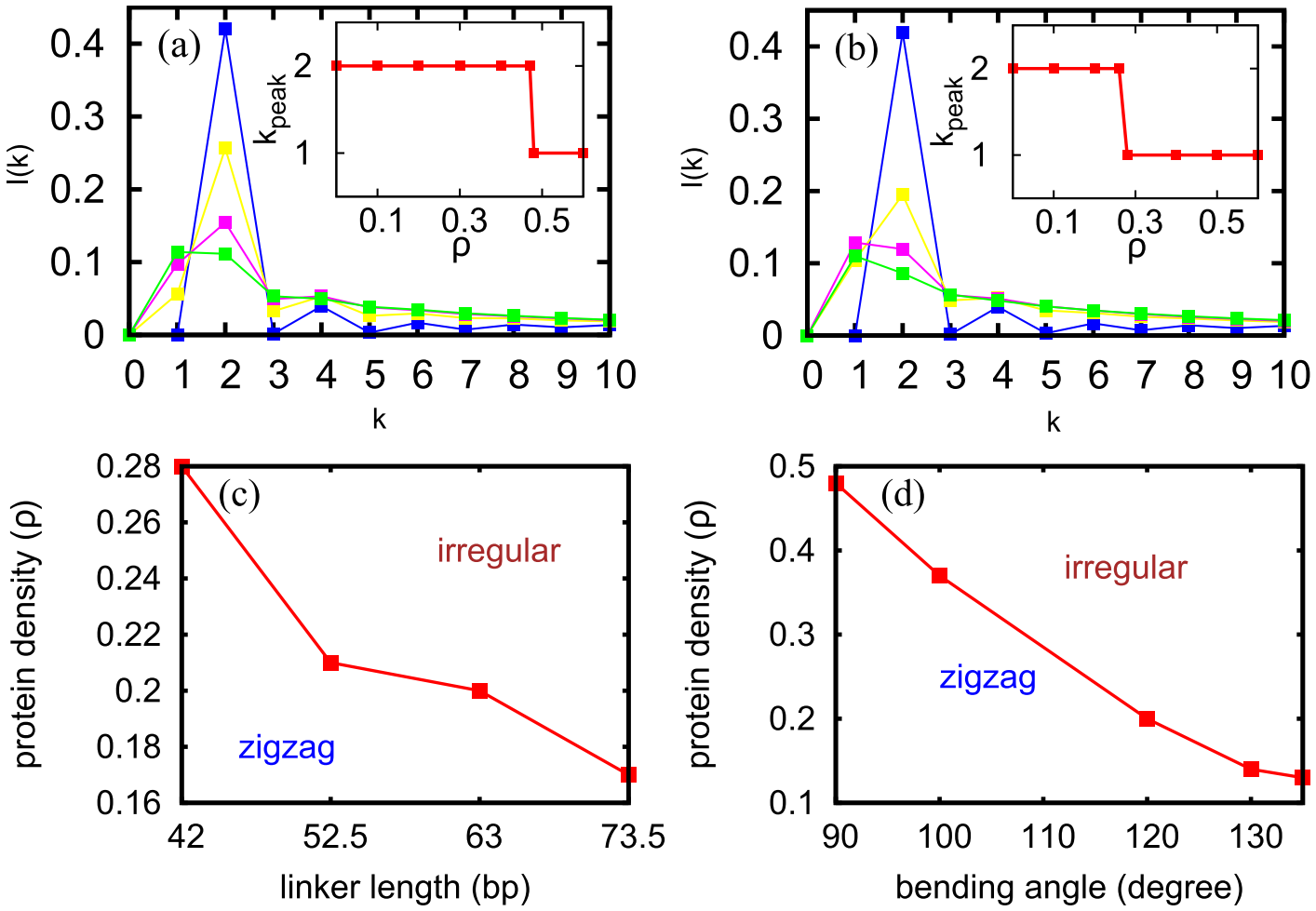

Fig 5. From 3D FRC model with 2000 nucleosomes. (a) $I(k)$ without any non-histone proteins (blue curve) and with different densities of non-histone proteins: $\rho = 0.1$ (yellow), $\rho = 0.3$ (pink), and $\rho = 0.5$ (green). The peak at $k = 2$ is shifted to $k = 1$ on increasing ρ. Here, the bending angle of the non-histone protein is $\theta_p = 90^\circ$ representing nhp6 and HMG-B. Inset: the peak location (k value at which $I(k)$ is peaked), k_{peak}, for different ρ. This indicates a transition from a zig-zag to an irregular structure. (b) The same as (a) but with θ_p chosen randomly from 90°–135° (c) A phase diagram obtained by varying the linker length and the density of proteins in the linker region (θ_p as in (b)). The red dots represent the values of the parameters at which the transition from zig-zag to irregular structure happens (i.e., parameter values at which $I(1) = I(2)$). (d) A similar phase diagram obtained by varying the bending angle (representing different proteins) and the protein density (linker length = 42*bp*).

doi:10.1371/journal.pcbi.1005365.g005

and $i/i + 2$ contacts [60]. Given that, in reality, there are proteins of different types binding in a heterogeneous manner (e.g. LEF1: 107°-127°, nhp6: 120°) we repeated the calculation for different set of bending angles—angles randomly chosen from a range between 90° and 135° [56, 59]. The results are shown in Fig 5b. Here too the inset shows a transition from zig-zag to irregular structure as a function of protein density. In both the figures here, the chromatin becomes irregular when $\rho < 0.5$(at $\rho = 0.48$ in Fig 5a and $\rho = 0.28$ in Fig 5b). This is equivalent to having one non-histone protein for every four nucleosomes ($\approx 1/0.28$) or two nucleosomes ($\approx 1/0.48$), consistent with abundance of non-histone proteins in the cell [35]. It is known that there exists roughly one HMG protein for every two nucleosomes [35] and hence such irregular structures can be expected for chromatin in which nearly all available HMGB proteins bind at linker regions.

Phase diagram: Protein density, diversity and linker lengths

Even though the typical chromatin linker length (L_l) is rarely larger than the persistence length (L_p), it has been argued that the linker length variation may affect the structure of chromatin [32, 47, 61, 62]. We did FRC simulations for chromatin having different L_l values (see S10 Fig). For large L_l, $I(2)$ decreases considerably; however given that the largest biologically relevant L_l values ($\approx$ 70 bp) are much smaller than the L_p of DNA, $I(2)$ still remains dominant. We find that as L_l increases the ρ required to create irregular structures becomes smaller. We systematically investigated how the two variables—non-histone protein density and linker length—decide the structure of the chromatin. The result is summarized in a phase diagram shown in Fig 5c. For every value of linker length, we have a "critical" protein density beyond which the chromatin structure is irregular. This prediction can be tested *in vitro* by varying nucleosome density and protein density appropriately. We also did simulations of chromatin having non-uniform linker lengths (L_l taken from a distribution), and it also gave similar results (see S3 Text and S11 Fig). We then computed how different types of proteins, having different bending angles, will affect the phase diagram (see Fig 5d). We varied the bending angles in the range of 90°–135° (see S12 Fig), since this is the range in which most of the relevant non-histone proteins bend DNA. As expected, the more the bending angle, the less the density of protein that is required to make the chromatin structure irregular.

We studied a few other aspects as well: (i) Varied the angle induced by the nucleosomes (α_n) and examined its effect (see S13 Fig). (ii)Examined whether the zig-zag or non-histone protein-bound chromatin have a fractal nature [22, 63, 64], and how non-histone proteins would affect packing ratio (R_g) (see S4 Text and S14 Fig). (iii) Varied the histone tail interactions (the number of interacting tails and strength) and found how nucleosome contact map might alter in highly interacting regions (heterochromatin) vs loosely interacting regions (euchromatin) (see S2, S3 and S4 Figs).

Discussion

In this work we examined the role of DNA-bending non-histone proteins in determining the higher order structure of chromatin. Using computer simulations we show that the presence of non-histone proteins will destroy any regular structure of chromatin. We studied a few specific cases of proteins (e.g., HMG, nhp6) that bend DNA by sharp angles in the range 90°–135°. Our study suggests that the structure of chromatin, at the length scale of a few genes (kilobases to megabases) in particular, will be influenced by non-histone proteins that bind and bend DNA. We quantified the influence by computing neighbor contact probabilities for various parameter values.

Given that various DNA-bending proteins are abundant in nearly all cell types, it is imperative that the role of non-histone proteins be studied in detail for understanding the higher order structure. Estimates show that the total number of DNA-bending proteins in the HMG family alone will be roughly half the number of nucleosomes present in the cell [35]. This implies that half of the linker region could be potentially bent. Our study suggests that even when 28% to 48% (depending on the types of proteins present) of the linker regions are bent, the regular 30 nm structure will be destroyed, and we expect to see an irregular structure. A direct prediction of our study is that, even though the regular order is destroyed, there will be a good fraction of nucleosomes that would maintain contacts either with neighbors ($i/i+1$ contacts) or with next neighbors ($i/i+2$ contacts) (see Fig 5). This may be one way of differentiating the irregularity in chromatin structure arising from DNA-bending when compared to the irregularity that may arise due to other reasons such

as crowding. Recent Micro-C experiments [60] point precisely in this direction—absence of regular structure with existence of $i/i+1$ and $i/i+2$ contacts.

Our use of a coarse-grained description—FRC model—has an advantage that we do not have to use any microscopic parameters that are difficult to measure. We have only limited number of parameters: entry/exit angle that a nucleosome makes, typical linker lengths, range of angles over which the DNA is bent by non-histone proteins, and the density of non-histone proteins. Since we have some rough estimates of the first three parameters, the only one parameter we have to systematically vary is the density of non-histone proteins. Our results show that irrespective of the precise value of other parameters, chromatin becomes irregular once there are bound non-histone proteins above a critical density in the range ≈ 0.28–0.48 per linker region.

In this work we have assumed that non-histone proteins bind along the DNA with a certain probability (equivalently certain density). It is an interesting question how the results would get affected if the dynamics of the proteins are accounted [65]. Since binding and dissociation rates would add more parameters into the model, a simulation with non-histone protein dynamics is beyond the scope of the current work. We also do not know much about the binding specificity of these non-histone proteins. Hence it is also open to investigate how the results might alter if non-histone proteins like HMG have specific affinity to certain sequences. We have also not accounted for explicit molecular structure of non-histone proteins and linker histones [49] in the model. Since the computational cost of including various molecular details will be very high, a study of a long chromatin with many nucleosomes will only be possible with coarse-grained descriptions as we have done here. We hope future studies would tell us how much molecular details are crucial and how much of coarse-graining can be done without actually affecting the observable behaviour of the system.

Suggestion for new experiments to test our prediction

Our predictions may be tested in a few different ways. One may perform an *in vitro* experiment reconstituting chromatin in the presence of DNA bending proteins [13, 14, 66, 67]. The DNA-bending proteins are expected to destroy any regular zig-zag structure otherwise seen in the absence of non-histone proteins. Another way would be to perform Micro-C experiments (like Hseig et al [60]) by mutating DNA-bending proteins like nhp6. The prediction is that, when the dominant DNA-bending proteins are mutated, the next neighbour contact probability value will increase. One may also map the positions of DNA-bending proteins such as HMG and correlate them with Micro-C (Hi-C) data so that one obtains a better picture of how the non-histone proteins influence the 3D chromatin structure.

To conclude, in this work, we indicated the importance of non-histone proteins in determining the higher order structure and quantified the contribution of DNA-bending in generating irregular structures. We show that non-histone protein binding with biologically relevant proportions can create chromatin structures with equal fraction of next-neighbor $(i+2)$ and neighbor $(i+1)$ nucleosome interactions, as observed in recent experiments. Our work provides insights into understanding local chromatin structure (in the length scale of a few genes), which is crucial for studying phenomena like histone-modification spreading, accessibility of regulatory regions, and gene regulation in general. We must also acknowledge the role of other factors: in reality, the structure of chromatin will be determined not just by the non-histone proteins but by an interplay between different factors such as crowding, linker length variations, concentration of various ions (e.g Mg++), DNA-bending proteins, and other constituents [30–32]. We hope that this work will trigger more computational and experimental studies in future to probe this aspect more quantitatively, and delineate the relative contributions of all these factors in great detail.

Supporting information

S1 Text. Model. In this test we describe the model that considers nucleosomes as angle-inducing proteins. We also describe model for different sizes of non-histone proteins in this text.
(PDF)

S2 Text. Contact probability $I(k)$. This text describes definition and formula of contact probability.
(PDF)

S3 Text. Probability distribution formula for variable DNA linker length.
(PDF)

S4 Text. Chromatin: An irregular structure with fractal nature?.
(PDF)

S1 Table. BD: Parameter description.
(PDF)

S2 Table. Non-dimensional parameters.
(PDF)

S1 Fig. BD: different non-histone proteins bending DNA. Straight linker DNA, and linker DNA bent by proteins. Some non-histone proteins make angle between 2 bonds (size $\approx 20bp$) and some non-histone proteins make angle between 3 bonds (size $\approx 30bp$). Note that since our basic bond sizes are 10.5 bp (helical repeat), we do not have resolution below this length-scale.
(EPS)

S2 Fig. Chromatin configurations varying protein density and inter-nucleosomes strength. Snapshots of chromatin configurations for different parameters; (a), (b), (c) and (d): in the absence of non-histone proteins with non-dimensionalized inter-nucleosome interaction parameter $\tilde{k}_h = 0, 10, 30$ and 50 respectively; (e), (f), (g) and (h): in the presence of non-histone proteins—25% of the linker regions are bent due the binding of non-histone proteins. Similar to the case above, inter-nucleosome interaction are $\tilde{k}_h = 0, 10, 30$ and 50 respectively; (i), (j), (k) and (l): in the presence of non-histone proteins—50% of the linker regions are bent due to the binding of non-histone proteins. Similar to the case above, inter-nucleosome interaction are $\tilde{k}_h = 0, 10, 30$ and 50 respectively. One can see that the zig-zag nature is destroyed as we have more non-histone proteins.
(EPS)

S3 Fig. Contact probability $I(k)$ with high linker histone interaction. (a) $I(k)$ for high linker histone interaction $\tilde{k}_l = 100$, in the absence of non-histone proteins with inter-nucleosome interaction prameter $\tilde{k}_h = 0, 10, 30$ and 50. (b) and (c) $I(k)$, in the presence of non-histone proteins—25% and 50% of the linker regions are bent due to the binding of non-histone proteins respectively.
(EPS)

S4 Fig. Contact probability considering 4 interacting histone tails. (a) $I(k)$, with inter-nucleosome interactions ($\tilde{k}_h = 50$) where we vary the number of interacting histone tails (2 or 4 interacting tails for each nucleosome); fig (a) is in the absence of any non-histone protein. (b) The same in the presence of non-histone proteins binding and bending 50% of DNA linker regions. As the number of interacting tails increase, each nucleosome can interact with more neighbors.
(EPS)

S5 Fig. 3D configurations and contact probabilities considering linker histones explicitly. (a) Snapshot of chromatin structure (zigzag) in the absence of non-histone proteins, with inter-nucleosome interactions ($\tilde{k}_h = 50$). (b) Snapshot of chromatin structure in the presence of non-histone proteins binding 50% of DNA linker regions with inter-nucleosome interactions ($\tilde{k}_h = 50$). (c) $I(k)$ in the absence of any non-histone protein. (d) The same in the presence of non-histone proteins binding and bending 50% of DNA linker regions.
(EPS)

S6 Fig. 3D configurations and contact probabilities considering nucleosomes as angle-inducing proteins. (a) Snapshot of chromatin structure (zigzag) in the absence of non-histone proteins, with inter-nucleosome interactions ($\tilde{k}_h = 50$). (b) Snapshot of chromatin structure in the presence of non-histone proteins binding 50% of DNA linker regions with inter-nucleosome interactions ($\tilde{k}_h = 50$). (c) $I(k)$ without ($\tilde{k}_h = 0$) and with inter-nucleosome interactions ($\tilde{k}_h = 10, 30, 50$) and in the absence of any non-histone protein (d) Non-histone proteins bend linker region with θ_p = 120˚ with ($\tilde{k}_h = 0, 10, 30, 50$). Non-histone density is 0.5—that is they bind 50% of DNA linker regions. (e) Non-histone proteins bend linker region with θ_p = 90˚ with ($\tilde{k}_h = 0, 10, 30, 50$). Non-histone density is 0.5—that is they bind 50% of DNA linker regions. All the results are for the case where proteins make angle involving two bonds (i.e., protein size≈ 20bp; see Model section above).
(EPS)

S7 Fig. Contact probability $I(k)$ for different non-histone proteins having different bending angles. Non-histone proteins bend linker region with different angles θ_p = 60˚, 90˚, 120˚, 130˚, 135˚ and 150˚ with ($\tilde{k}_h = 50$). Non-histone density is 0.5. All the results are for the case where proteins make angle involving two bonds(i.e., protein size≈ 20bp; see Model section above).
(EPS)

S8 Fig. Non-histone proteins having different bending angles with a longer size. $I(k)$ with non-histone proteins that make angle involving three bonds(i.e., protein size≈ 30bp; see Model section above) (a) non-histone proteins bend linker region $\tilde{r}_p = 2r_s$ (equivalent to θ_p = 120˚) with ($\tilde{k}_h = 0, 10, 30, 50$). (b) The same for $\tilde{r}_p = 2.4r_s$ (equivalent to θ_p = 90˚) with ($\tilde{k}_h = 0, 10, 30, 50$). All for the case of non-histone proteins binding 50% of DNA linker regions (i. e. protein density ρ = 0.5). Compare these with $I(k)$ in S6 Fig for a similar case with proteins of a smaller size.
(EPS)

S9 Fig. Using Morse potential for inter-nucleosome interactions. $I(k)$, with inter-nucleosome interactions using harmonic ($\tilde{k}_h = 50$) and Morse potentials with comparable parameters. (a) $I(k)$ in the absence of any non-histone protein (b) The same in the presence of non-histone proteins binding 50% of DNA linker regions. See the Model part in S1 Text; Morse potential parameters are chosen such that $\tilde{k}_h = 50$ matches with spring constant of the harmonic interaction.
(EPS)

S10 Fig. Contact probability $I(k)$ for different DNA-bending angles. Results from 3D FRC model (M = 2000 nucleosomes) for specific bending angles (a) 100˚ (b) 120˚ (c) 130˚ (d) 135˚. Inset in all figures: curve between probability (density) of non-histone protein binding (ρ) and k at which $I(k)$ is peaking (k_{peak}), indicating the transition from zig-zag to an irregular structure.
(EPS)

S11 Fig. Contact probability $I(k)$ for different DNA linker lengths. Results from 3D FRC model (M = 2000 nucleosomes) with and without non-histone proteins for different linker DNA lengths (a), (b), (c), and (d): Main figures depict I(k) for linker lengths 42 bp, 52.5 bp, 63 bp, and 73.5 bp, respectively. The blue curves are the results obtained without any non-histone proteins. Other curves are for different non-histone protein densities given by $\rho = 0.1$ (yellow), $\rho = 0.25$ (pink), and $\rho = 0.5$ (green). Inset in all figures: curve between probability (density) of non-histone protein binding (ρ) and k at which $I(k)$ is peaking (k_{peak}), indicating the transition from zig-zag to an irregular structure as discussed in the main text. In all these figures, bending angles are chosen randomly between 90 and 135 degrees. Different linker lengths may arise due to heterogeneity; nucleosome free regions may also be formed with the help of enzymes that bind and remove nucleosomes.
(EPS)

S12 Fig. Structure and contact probability $I(k)$ for variable DNA linker length. (a) Configuration of chromatin (M = 50 nucleosomes) with variable linker length (31.5 bp to 73.5 bp) such that the average linker length is 42bp; note the zig-zag nature of the structure. (b) Configuration of chromatin in the presence of non-histone protein bound in 25% of the linker regions with variable linker length. Both these configurations are plotted from the FRC data (angle randomly selected from a uniform distribution between 90–135 degrees). (c) Calculation of $I(k)$ (M = 2000 nucleosomes) for variable linker length (31.5 bp to 73.5 bp; average 42bp) without any bound non-histone protein (blue curve) and with different probability of having non-histone proteins: $\rho = 0.1$ (yellow), $\rho = 0.25$ (pink), and $\rho = 0.5$ (green).
(EPS)

S13 Fig. Effect of nucleosome-angle (α_n) on chromatin structure. Certain proteins (H1 or other nucleosome binding proteins) may influence the DNA entry/exit angle (α_n; see model section above) induced by nucleosomes. Here we plot the peak value of $I(k)$ on changing α_n. Zigzag is destroyed for large nucleosome's angle.
(EPS)

S14 Fig. End to end distances and radius of gyration of chromatin as a function of contour length. (a) RMS end-to-end distance (in bp) as a function of the total number of vectors (links) in the 3D FRC chromatin, for two cases: without ($\rho = 0$) and with ($\rho = 0.3$) non-histone proteins. The red lines represent $R_{\rm rms} \propto N$ and the green lines represent $R_{\rm rms} \propto N^{0.5}$. The results suggests that non-histone proteins make the chromatin irregular even at very small length scales. (b) Radius of gyration (R_g in bp) as a function of number of nucleosomes (M). It is interesting to note that non-histone proteins reduce R_g and hence increases the packing ratio of the chromatin.
(EPS)

Acknowledgments

We acknowledge communication with Oliver Rando in which he told us about the role of nhp6 and how Micro-C experiments with nhp6 mutants may potentially test our predictions. We thank Craig Peterson and Michael Poirier for useful discussions and in particular discussion on chromatin reconstitution experiments. We also thank Santanu Ghosh, Geeta Narlikar, G. V. Shivashankar, John Marko, Wendy Bickmore, Jyotsana J. Parmar, Hungyo Kharerin and Srivastav Ranganathan for useful discussions.

Author contributions

Conceptualization: GB IJ DD MMI RP.

Data curation: GB IJ.

Funding acquisition: RP.

Investigation: GB IJ DD MMI RP.

Methodology: RP DD MMI GB IJ.

Supervision: RP DD MMI.

Writing – original draft: GB DD MMI RP.

Writing – review & editing: GB IJ DD MMI RP.

References

1. Holde KEV. Chromatin. Springer Science & Business Media; 2012.
2. Tremethick DJ. Higher-Order Structures of Chromatin: The Elusive 30 nm Fiber. Cell. 2007; 128 (4):651–654. doi: 10.1016/j.cell.2007.02.008 PMID: 17320503
3. Bian Q, Belmont AS. Revisiting higher-order and large-scale chromatin organization. Current opinion in cell biology. 2012; 24(3):1–8. doi: 10.1016/j.ceb.2012.03.003
4. Zhu P, Li G. Structural insights of nucleosome and the 30-nm chromatin fiber. Curr Opin Struct Biol. 2016; 36:106–115. doi: 10.1016/j.sbi.2016.01.013 PMID: 26872330
5. Widom J, Klug A. Structure of the 300A chromatin filament: X-ray diffraction from oriented samples. Cell. 1985; 43(1):207–213. doi: 10.1016/0092-8674(85)90025-X PMID: 4075395
6. Finch JT, Klug A. Solenoidal model for superstructure in chromatin. Proc Natl Acad Sci U S A. 1976; 73 (6):1897–1901. doi: 10.1073/pnas.73.6.1897 PMID: 1064861
7. Robinson PJJ, Fairall L, Huynh VAT, Rhodes D. EM measurements define the dimensions of the 30-nm chromatin fiber: Evidence for a compact, interdigitated structure. Proc Natl Acad Sci U S A. 2006; 103 (17):6506–6511. doi: 10.1073/pnas.0601212103 PMID: 16617109
8. Horowitz RA, Agard DA, Sedat JW, Woodcock CL. The three-dimensional architecture of chromatin in situ: Electron tomography reveals fibers composed of a continuously variable zig-zag nucleosomal ribbon. J Cell Biol. 1994; 125(1):1–10. doi: 10.1083/jcb.125.1.1 PMID: 8138564
9. Woodcock CL, Frado LL, Rattner JB. The higher-order structure of chromatin: evidence for a helical ribbon arrangement. J Cell Biol. 1984; 99(1 Pt 1):42–52. doi: 10.1083/jcb.99.1.42 PMID: 6736132
10. Pehrson JR. Probing the Conformation of Nucleosome Linker DNA in Situ with Pyrimidine Dimer Formation. Journal of Biological Chemistry. 1995; 270(38):22440–22444. PMID: 7673231
11. Rydberg B, Holley WR, Mian IS, Chatterjee A. Chromatin conformation in living cells: support for a zig-zag model of the 30 nm chromatin fiber. Journal of Molecular Biology. 1998; 284(1):71–84. doi: 10.1006/jmbi.1998.2150 PMID: 9811543
12. Song F, Chen P, Sun D, Wang M, Dong L, Liang D, et al. Cryo-EM study of the chromatin fiber reveals a double helix twisted by tetranucleosomal units. Science. 2014; 344(6182):376–380. doi: 10.1126/science.1251413 PMID: 24763583
13. Schalch T, Duda S, Sargent D, Richmond T. X-ray structure of a tetranucleosome and its implications for the chromatin fibre. Nature. 2005; 436(7047):138–141. doi: 10.1038/nature03686 PMID: 16001076
14. Dorigo B, Schalch T, Kulangara A, Duda S, Schroeder RR, Richmond TJ. Nucleosome arrays reveal the two-start organization of the chromatin fiber. Science. 2004; 306(5701):1571–1573. doi: 10.1126/science.1103124 PMID: 15567867
15. Gerchman SE, Ramakrishnan V. Chromatin higher-order structure studied by neutron scattering and scanning transmission electron microscopy. Proc Natl Acad Sci U S A. 1987; 84(22):7802–7806. doi: 10.1073/pnas.84.22.7802 PMID: 3479765
16. Holde KV, Zlatanova J. Chromatin higher order structure: Chasing a Mirage? J Biol Chem. 1995; 270 (15):8373–8376. doi: 10.1074/jbc.270.15.8373 PMID: 7721727
17. Maeshima K, Hihara S, Eltsov M. Chromatin structure: Does the 30-nm fibre exist in vivo? Curr Opin Cell Biol. 2010; 22(3):291–297. doi: 10.1016/j.ceb.2010.03.001 PMID: 20346642

18. Fussner E, Ching RW, Bazett-Jones DP. Living without 30nm chromatin fibers. Trends Biochem Sci. 2011; 36(1):1–6. doi: 10.1016/j.tibs.2010.09.002 PMID: 20926298

19. Razin SV, Gavrilov AA. Chromatin without the 30-nm fiber: constrained disorder instead of hierarchical folding. Epigenetics. 2014; 9(5):653–657. doi: 10.4161/epi.28297 PMID: 24561903

20. Scheffer MP, Eltsov M, Frangakis AS. Evidence for short-range helical order in the 30-nm chromatin fibers of erythrocyte nuclei. Proc Natl Acad Sci U S A. 2011; 108(41):16992–16997. doi: 10.1073/pnas.1108268108 PMID: 21969536

21. Eltsov M, Maclellan KM, Maeshima K, Frangakis AS, Dubochet J. Analysis of cryo-electron microscopy images does not support the existence of 30-nm chromatin fibers in mitotic chromosomes in situ. Proc Natl Acad Sci U S A. 2008; 105(50):19732–19737. doi: 10.1073/pnas.0810057105 PMID: 19064912

22. Nishino Y, Eltsov M, Joti Y, Ito K, Takata H, Takahashi Y, et al. Human mitotic chromosomes consist predominantly of irregularly folded nucleosome fibres without a 30-nm chromatin structure. EMBO J. 2012; 31(7):1644–1653. doi: 10.1038/emboj.2012.35 PMID: 22343941

23. Bouchet-Marquis C, Dubochet J, Fakan S. Cryoelectron microscopy of vitrified sections: a new challenge for the analysis of functional nuclear architecture. Histochem Cell Biol. 2006; 125(1–2):43–51. doi: 10.1007/s00418-005-0093-x PMID: 16328430

24. Maeshima K, Eltsov M. Packaging the Genome: the Structure of Mitotic Chromosomes. J Biochem. 2008; 143(2):145–153. doi: 10.1093/jb/mvm214 PMID: 17981824

25. Woodcock CL, Grigoryev SA, Horowitz RA, Whitaker N. A chromatin folding model that incorporates linker variability generates fibers resembling the native structures. Proc Natl Acad Sci U S A. 1993; 90 (19):9021–9025. doi: 10.1073/pnas.90.19.9021 PMID: 8415647

26. Bednar J, Horowitz RA, Grigoryev SA, Carruthers LM, Hansen JC, Koster AJ, et al. Nucleosomes, linker DNA, and linker histone form a unique structural motif that directs the higher-order folding and compaction of chromatin. Proceedings of the National Academy of Sciences. 1998; 95(24):14173–14178. doi: 10.1073/pnas.95.24.14173

27. Marko JF. Introduction to Single-DNA Micromechanics. In: Les Houches Session LXXXII: Multiple Aspects of DNA and RNA from Biophysics to Bioinformatics. Elsevier; 2005. p. 211–270.

28. Thoma F, Koller T, Klug A. Involvement of histone H1 in the organization of the nucleosome and of the salt-dependent superstructures of chromatin. The Journal of Cell Biology. 1979; 83(2):403–427. doi: 10.1083/jcb.83.2.403 PMID: 387806

29. Maeshima K, Imai R, Tamura S, Nozaki T. Chromatin as dynamic 10-nm fibers. Chromosoma. 2014; 123(3):225–237. doi: 10.1007/s00412-014-0460-2 PMID: 24737122

30. Grigoryev SA, Arya G, Correll S, Woodcock CL, Schlick T. Evidence for heteromorphic chromatin fibers from analysis of nucleosome interactions. Proc Natl Acad Sci U S A. 2009; 106(32):13317–13322. doi: 10.1073/pnas.0903280106 PMID: 19651606

31. Kruithof M, Chien FT, Routh A, Logie C, Rhodes D, van Noort J. Single-molecule force spectroscopy reveals a highly compliant helical folding for the 30-nm chromatin fiber. Nat Struct Mol Biol. 2009; 16 (5):534–540. doi: 10.1038/nsmb.1590 PMID: 19377481

32. Perisic O, Collepardo-Guevara R, Schlick T. Modeling studies of chromatin fiber structure as a function of DNA linker length. J Mol Biol. 2010; 403(5):777–802. doi: 10.1016/j.jmb.2010.07.057 PMID: 20709077

33. Schiessel H, Gelbart WM, Bruinsma R. DNA Folding: Structural and Mechanical Properties of the Two-Angle Model for Chromatin. Biophysical Journal. 2001; 80(4):1940–1956. doi: 10.1016/S0006-3495(01)76164-4 PMID: 11259307

34. Stillman DJ. Nhp6: A small but powerful effector of chromatin structure in Saccharomyces cerevisiae. Biochimica et Biophysica Acta (BBA)—Gene Regulatory Mechanisms. 2010; 1799(1–2):175–180.

35. Kuehl L, Salmond B, Tran L. Concentrations of high-mobility-group proteins in the nucleus and cytoplasm of several rat tissues. J Cell Biol. 1984; 99(2):648–654. doi: 10.1083/jcb.99.2.648 PMID: 6235236

36. Giese K, Cox J, Grosschedl R. The HMG domain of lymphoid enhancer factor 1 bends DNA and facilitates assembly of functional nucleoprotein structures. Cell. 1992; 69(1):185–195. doi: 10.1016/0092-8674(92)90129-Z PMID: 1555239

37. Paull TT, Haykinson MJ, Johnson RC. The nonspecific DNA-binding and -bending proteins HMG1 and HMG2 promote the assembly of complex nucleoprotein structures. Genes Dev. 1993; 7(8):1521–1534. doi: 10.1101/gad.7.8.1521 PMID: 8339930

38. Thomas JO, Travers AA. HMG1 and 2, and related'architectural' DNA-binding proteins. Trends Biochem Sci. 2001; 26(3):167–174. doi: 10.1016/S0968-0004(01)01801-1 PMID: 11246022

39. Cloutier TE, Widom J. Spontaneous Sharp Bending of Double-Stranded DNA. Mol Cell. 2004; 14 (3):355–362. doi: 10.1016/S1097-2765(04)00210-2 PMID: 15125838

40. Yan J, Marko JF. Localized Single-Stranded Bubble Mechanism for Cyclization of Short Double Helix DNA. Phys Rev Lett. 2004; 93(10):108108. doi: 10.1103/PhysRevLett.93.108108 PMID: 15447460

41. Yan J, Kawamura R, Marko JF. Statistics of loop formation along double helix DNAs. Phys Rev E Stat Nonlin Soft Matter Phys. 2005; 71(6 Pt 1):061905. doi: 10.1103/PhysRevE.71.061905 PMID: 16089763

42. Wiggins PA, Nelson PC. Generalized theory of semiflexible polymers. Phys Rev E. 2006; 73 (3):031906. doi: 10.1103/PhysRevE.73.031906

43. Ranjith P, Kumar PBS, Menon GI. Distribution Functions, Loop Formation Probabilities, and Force-Extension Relations in a Model for Short Double-Stranded DNA Molecules. Phys Rev Lett. 2005; 94 (13):138102. doi: 10.1103/PhysRevLett.94.138102 PMID: 15904042

44. Langowski J. Polymer chain models of DNA and chromatin. Eur Phys J E Soft Matter. 2006; 19(3):241–249. doi: 10.1140/epje/i2005-10067-9 PMID: 16547610

45. Arya G, Schlick T. Role of histone tails in chromatin folding revealed by a mesoscopic oligonucleosome model. Proc Natl Acad Sci U S A. 2006; 103(44):16236–16241. doi: 10.1073/pnas.0604817103 PMID: 17060627

46. Diesinger P, Kunkel S, Langowski J, Heermann D. Histone Depletion Facilitates Chromatin Loops on the Kilobasepair Scale. Biophysical Journal. 2010; 99(9):2995–3001. doi: 10.1016/j.bpj.2010.08.039 PMID: 21044597

47. Collepardo-Guevara R, Schlick T. Chromatin fiber polymorphism triggered by variations of DNA linker lengths. Proc Natl Acad Sci U S A. 2014; 111(22):8061–8066. doi: 10.1073/pnas.1315872111 PMID: 24847063

48. Katritch V, Bustamante C, Olson WK. Pulling chromatin fibers: computer simulations of direct physical micromanipulations1. Journal of Molecular Biology. 2000; 295(1):29–40. doi: 10.1006/jmbi.1999.3021 PMID: 10623506

49. Zhou BR, Jiang J, Feng H, Ghirlando R, Xiao T, Bai Y. Structural Mechanisms of Nucleosome Recognition by Linker Histones. Molecular Cell. 2015; 59(4):628–638. doi: 10.1016/j.molcel.2015.06.025 PMID: 26212454

50. Netz R. Nonequilibrium Unfolding of Polyelectrolyte Condensates in Electric Fields. Phys Rev Lett. 2003; 90(12):128104. doi: 10.1103/PhysRevLett.90.128104 PMID: 12688907

51. Plimpton S. Fast Parallel Algorithms for Short-Range Molecular Dynamics. Journal of Computational Physics. 1995; 117(1):1–19. doi: 10.1006/jcph.1995.1039

52. Kruppa M, Moir RD, Kolodrubetz D, Willis IM. Nhp6, an {HMG1} Protein, Functions in {SNR6} Transcription by {RNA} Polymerase {III} in S. cerevisiae. Molecular Cell. 2001; 7(2):309–318. doi: 10.1016/S1097-2765(01)00179-4 PMID: 11239460

53. Belgrano FS, de Abreu da Silva IC, Bastos de Oliveira FM, Fantappie MR, Mohana-Borges R. Role of the Acidic Tail of High Mobility Group Protein B1 (HMGB1) in Protein Stability and DNA Bending. PLoS ONE. 2013; 8(11). doi: 10.1371/journal.pone.0079572 PMID: 24255708

54. Yamakawa H. Helical Wormlike Chains in Polymer Solutions. 1st ed. Springer-Verlag Berlin Heidelberg; 1997.

55. Humphrey W, Dalke A, Schulten K. VMD—Visual Molecular Dynamics. J Mol Graph. 1996; 14:33–38. doi: 10.1016/0263-7855(96)00018-5 PMID: 8744570

56. Yen YM, Li X, Case DA, Giese K, Crosschedl R, Giese K, et al. Determinants of DNA binding and bending by the Saccharomyces cerevisiae high mobility group protein NHP6A that are important for its biological activities. Role of the unique N terminus and putative intercalating methionine. J Biol Chem. 1998; 273(8):4424–4435. doi: 10.1074/jbc.273.8.4424 PMID: 9468494

57. Allain FHT, Yen YM, Masse JE, Schultze P, Dieckmann T, Johnson RC, et al. Solution structure of the HMG protein NHP6A and its interaction with DNA reveals the structural determinants for non-sequence-specific binding. The EMBO Journal. 1999; 18(9):2563–2579. doi: 10.1093/emboj/18.9.2563 PMID: 10228169

58. Lorenz M, Hillisch A, Payet D, Buttinelli M, Travers A, Diekmann S. DNA Bending Induced by High Mobility Group Proteins Studied by Fluorescence Resonance Energy Transfer. Biochemistry. 1999; 38 (37):12150–12158. doi: 10.1021/bi990459+ PMID: 10508419

59. Love JJ, Wong B, Johnson RC, Giese K, Crosschedl R, Giese K, et al. Structural basis for DNA bending by the architectural transcription factor {LEF-1}. Nature. 1995; 376(6543):791–795. doi: 10.1038/376791a0 PMID: 7651541

60. Hsieh TH, Weiner A, Lajoie B, Dekker J, Friedman N, Rando O. Mapping Nucleosome Resolution Chromosome Folding in Yeast by Micro-C. Cell. 2015; 162(1):108–119. doi: 10.1016/j.cell.2015.05.048 PMID: 26119342

61. Correll SJ, Schubert MH, Grigoryev SA. Short nucleosome repeats impose rotational modulations on chromatin fibre folding. EMBO J. 2012; 31(10):2416–2426. doi: 10.1038/emboj.2012.80 PMID: 22473209

62. Schlick T, Hayes J, Grigoryev S. Toward Convergence of Experimental Studies and Theoretical Modeling of the Chromatin Fiber. J Biol Chem. 2012; 287(8):5183–5191. doi: 10.1074/jbc.R111.305763 PMID: 22157002

63. Lieberman-Aiden E, van Berkum NL, Williams L, Imakaev M, Ragoczy T, Telling A, et al. Comprehensive Mapping of Long-Range Interactions Reveals Folding Principles of the Human Genome. Science. 2009; 326(5950):289–293. doi: 10.1126/science.1181369 PMID: 19815776

64. Bancaud A, Huet S, Daigle N, Mozziconacci J, Beaudouin J, Ellenberg J. Molecular crowding affects diffusion and binding of nuclear proteins in heterochromatin and reveals the fractal organization of chromatin. EMBO journal. 2009; 28(24):3785–3798. doi: 10.1038/emboj.2009.340 PMID: 19927119

65. Thomas JO, Stott K. H1 and HMGB1: modulators of chromatin structure. Biochemical Society Transactions. 2012; 40(2):341–346. doi: 10.1042/BST20120014 PMID: 22435809

66. Yang JG, Narlikar GJ. FRET-based methods to study ATP-dependent changes in chromatin structure. Methods. 2007; 41(3):291–295. doi: 10.1016/j.ymeth.2006.08.015 PMID: 17309839

67. Poirier MG, Oh E, Tims HS, Widom J. Dynamics and function of compact nucleosome arrays. Nat Struct Mol Biol. 2009; 16(9):938–944. doi: 10.1038/nsmb.1650 PMID: 19701201